

Sub-20 nm island self-organisation stimulated by spatially periodic laser exposure in the GaAs/InGaAs/GaAs epitaxial system

Yu.K. Verevkin, V.N. Petryakov, Yu.Yu. Gushchina, C.S. Peng, C. Tan, M. Pessa, Z. Wang, S.M. Olaizola, S. Tisserand

Abstract. Four-beam laser interference is shown to stimulate the self-organisation of periodic two-dimensional arrays of nanoislands on the surface of GaAs/InGaAs/GaAs epitaxial structures. (Self-organisation is here taken to mean processes that determine the island size.) The island size distribution has two well-defined maxima. The smaller islands (~ 5 nm) form inside each heat-affected zone, and the larger islands (~ 15 nm), at the periphery of such zones. The island width is a factor of 20–60 smaller than the standing wave period, which can be accounted for in terms of the elastic stress on the surface of the epitaxial film.

Keywords: nanoisland self-organisation, GaAs/InGaAs/GaAs epitaxy, spatially periodic laser exposure.

1. Introduction

Self-organisation has been extensively studied and is widely used to produce nanostructures and improve the performance of semiconductor lasers [1] and detectors. The self-organisation of nanostructures is also of interest in many areas of nanosystems science and for nanotechnology development [2].

Optimisation of the conditions for self-organisation of nanostructures on the surface of various materials remains the subject of intense research [3–7]. An important issue in this area is the ability to produce periodic arrays of islands less than 100 nm in size [8–13]. To this end, use is commonly made of various masks or prepatterned sub-

strates. Pedraza et al. [13] investigated the self-organisation of nanoislands on Si exposed to high-power UV light and attributed it to surface wave excitation. The self-organisation of the nanostructures was achieved after more than 200 pulses with an energy density of ~ 1 J cm⁻². Patella et al. [14] reported a detailed study of quantum dot self-organisation in the Si–Ge/Si and InAs/GaAs systems on flat and patterned substrates. An interesting effect was described by Lee et al. [15]: the formation of separate quantum dot clusters on InAs/GaAs. The parameters of the InAs quantum dots were controlled using ‘nanoholed island templates’ prepared by GaAs/GaAs droplet homoepitaxy [15, 16]. The generation of nanoholed islands on the substrate surface made it possible to confine the nucleation of quantum dots to the islands and to tune their morphology by varying the growth conditions. An alternative approach to confining the growth of quantum size effect islands on Si and GaAs single crystals was adopted by Verevkin et al. [17]: the crystals were exposed to four high-power coherent UV laser beams, which produced periodic arrays of islands and pits less than 100 nm in size.

This configuration was found to directly stimulate the growth of islands a factor of 5–10 smaller than the period of the resultant standing wave [17]. The effect cannot be accounted for only in terms of the dependence on the thermal threshold of laser exposure: it persisted when the incident energy density was increased almost twofold. If there is only thermal nonlinearity, interference maxima ten times smaller than the standing wave period can be obtained when the threshold is exceeded by less than 10%. To interpret the small island size, the assumption was made that the observed morphological changes were contributed by surface stress [17]. In this paper, we report surface nanostructuring results for the GaAs/InGaAs/GaAs epitaxial system, which further highlight the important role of surface stress in surface instability development.

2. Experimental and results

In our experiments, we used four types of samples on n-GaAs (001) single-crystal substrates. After removal of the oxide layer from the substrate surface, a GaAs buffer no more than 100 nm in thickness was deposited at 580 °C. Next, a 3-nm In_{0.35}Ga_{0.65}As layer was grown at 520 °C. The top GaAs layer, 5, 10, 20 or 40 nm thick, was also grown at 520 °C. In all the growth runs, we used a solid-source molecular beam epitaxy system.

Yu.K. Verevkin, V.N. Petryakov Institute of Applied Physics, Russian Academy of Sciences, ul. Ulyanova 46, 603950 Nizhnii Novgorod, Russia; e-mail: verevkin@appl.sci-nnov.ru;

Yu.Yu. Gushchina Research and Education Center for Physics of Solid State Nanostructures, Nizhnii Novgorod State University, prosp. Gagarina 23, 603950 Nizhnii Novgorod, Russia;

C.S. Peng, C. Tan, M. Pessa Optoelectronics Research Centre, Tampere University of Technology, Tampere, Finland;

Z. Wang Manufacturing Engineering Centre, Cardiff University, Cardiff, UK;

S.M. Olaizola CEIT and Tecnun (University of Navarra), San Sebastian, Spain;

S. Tisserand SILIOS Technologies, Peynier, France

Received 6 April 2009; revision received 3 August 2009

Kvantovaya Elektronika 40 (1) 73–76 (2010)

Translated by O.M. Tsarev

The light source was a XeCl laser (wavelength, 308 nm; coherence length over 30 cm) delivering up to 100 mJ of energy in a 10- to 15-ns pulse, with a near-diffraction-limited beam. All the results presented below were obtained in a single laser shot, using four-beam interference. The laser beam was split into four beams by three dielectric mirrors with 50 % reflectances. The beams were recombined on the sample surface using eight dielectric mirrors with $\sim 99\%$ reflectances. The polarisation of the beams was TE–TM in the notation proposed by Fernandez and Phillion [18], who also presented detailed analytical expressions and computed standing wave intensity profile for such systems. The profile is sinusoidal along the two coordinates in the sample plane.

All the nanostructuring experiments were carried out under normal conditions (the samples were mounted vertically). The morphological changes were independent of the GaAs film thickness to within the accuracy in our surface topography measurements. Below, we present the UV nanostructuring results for a 20-nm film.

Figure 1 presents an atomic force microscopy (AFM) image of the GaAs/InGaAs/GaAs surface after exposure to four laser beams with an average energy density of $\sim 1.5 \text{ J cm}^{-2}$. Note that, in that experiment, the bisectors of the angles between the beams propagating in the same plane of incidence were not normal to the sample surface, which caused the intensity of the interference maxima to vary by a factor of two [18] along the diagonal from top left to bottom right in Fig. 1. Therefore, with a single laser shot we were able to observe surface topography changes at a local energy density varied by a factor of two. Two features of the laser exposure results warrant attention. The area modified by a single interference maximum is nearly rectangular in shape, while the heat-affected zone has a

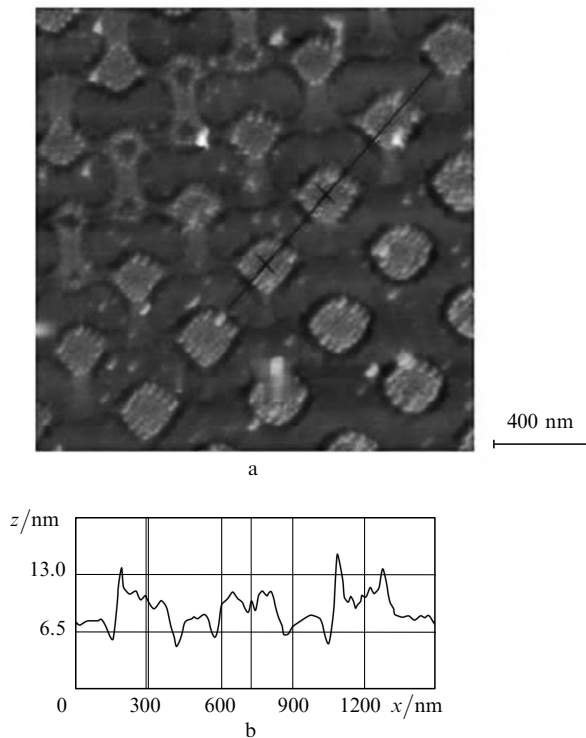


Figure 1. (a) AFM image of the GaAs/InGaAs/GaAs structure after exposure to four coherent XeCl laser beams; (b) height profile along the solid line in the image.

circular shape. Another important point is that this zone contains many islands, whereas there are no islands in the unexposed areas.

Figure 2 shows AFM images of the film at a magnification higher than that in Fig. 1. It is worth noting here that the epitaxial film differs in morphological changes from single crystals [17] and amorphous films [19–22]. In the case of crystals, a single island is formed near an interference maximum, with a hole in the immediate region of the maximum, which points to a material displacement process. Four-beam processing of amorphous films creates a hole at each intensity maximum, surrounded by an elevation, as in the case of an explosion. The AFM image in Fig. 3 was used to obtain statistical information about the island size. It is well seen that the islands produced in the peripheral part of the interference maximum (7–20 nm in diameter) differ markedly in size from those closer to the centre (3–8 nm). The corresponding island size distributions are presented in Figs 4 and 5. The density of the peripheral islands is $\sim 10^{10} \text{ cm}^{-2}$ and that of the inner islands is estimated at $5 \times 10^{10} \text{ cm}^{-2}$.

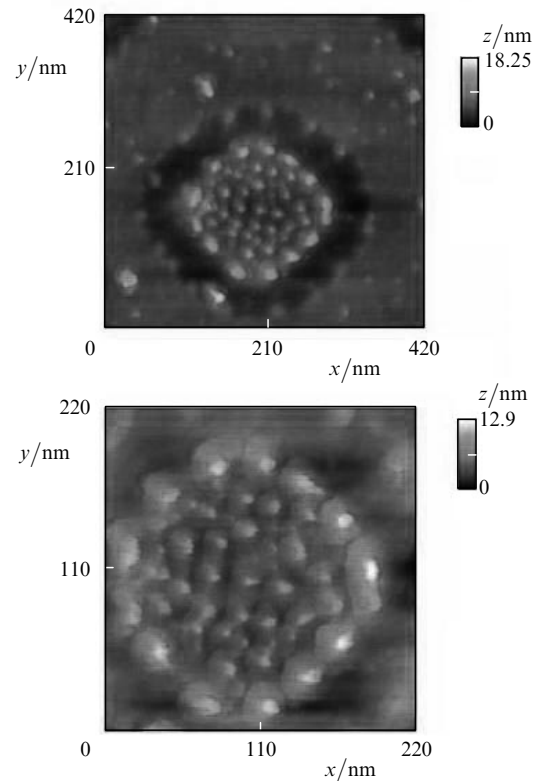


Figure 2. AFM images of different areas on the surface of the GaAs/InGaAs/GaAs structure, illustrating different island configurations.

3. Discussion

Based on the present results, we make a number of assumptions as to the physics of island formation. Note first of all that, under the conditions of our experiments, there is no ablation (no material removal from the surface being processed), and surface structuring is due to material displacement over the surface. The island width is a factor of 20–60 smaller than the standing wave period. Such dimensions cannot be accounted for only in terms of

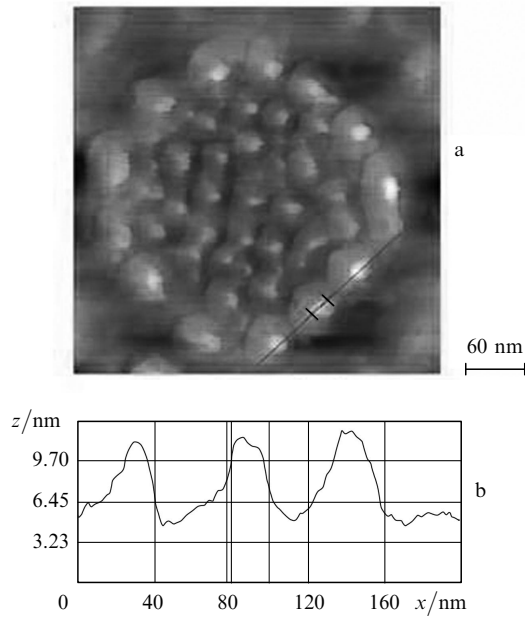


Figure 3. (a) AFM image of an area around an interference maximum; (b) height profile along the solid line in the image.

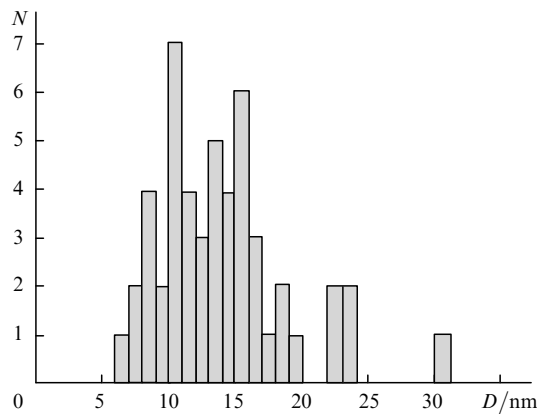


Figure 4. Size distribution of the peripheral (larger) islands.

thermal processes: similar islands grow when the incident laser fluence is increased twofold. As in the case of single crystals [17], taking into account the effect of surface stress

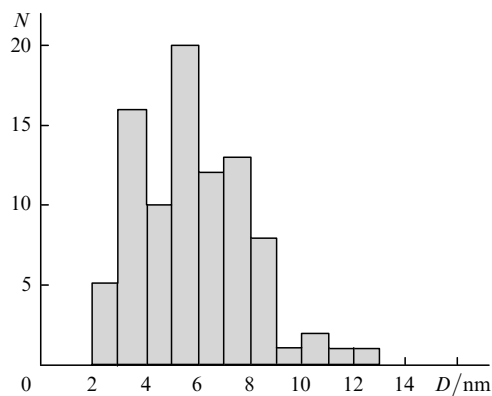


Figure 5. Size distribution of the inner (smaller) islands.

is crucial for understanding the islanding behaviour of epitaxial films. We believe that the island formation in our experiments can be interpreted in terms of Stranski–Krastanow growth.

It is well known that the surface of single crystals (as well as that of epitaxial films) is under mechanical stress. The surface stress arises from the fact that the bulk and surface atoms differ in environment, and is higher at a better surface quality of single crystals. The stress vanishes at surface defects which are generated during crystal growth and processing. Surface defects may include any known structural defects. Therefore, the length scale of stress variations depends on crystal quality and may be comparable to the sample size, as observed in studies of silicon single crystals [17].

The main source of surface stress in epitaxial films is also well known: lattice mismatch between the film ($C_I = 6.0584 \text{ \AA}$ in InAs) and the substrate ($C_G = 5.6534 \text{ \AA}$ in GaAs). The length scale of stress variations is therefore determined by the beating between two periodic functions with periods C_I and C_G . Under the simplest assumptions as to the minimum beat period, we obtain $2C_I C_G / (C_I - C_G)$. This estimate gives $\sim 170 \text{ \AA}$. In our experiments, the composition of the epitaxial film was $\text{In}_{0.35}\text{Ga}_{0.65}\text{As}$. Its lattice parameter can be evaluated under the assumption that C is a linear function of indium concentration. The beat period is then $\sim 510 \text{ \AA}$. This value is in astonishing agreement with the experimentally determined island spacing (Fig. 3), providing further evidence that surface stress had a significant effect on the nanostructuring of the epitaxial films in our experiments. We are thus led to a stronger assumption: the variation in island spacing is due to local indium concentration fluctuations.

4. Conclusions

We proposed and tested an effective approach for producing periodic two-dimensional arrays of sub-20 nm islands on the surface of epitaxial films. The process can be used to grow multilayer epitaxial structures with correlated quantum dots.

The described approach to the growth of periodic arrays of sub-20 nm islands may become an alternative to the use of various masks as a means of spatially confining the nucleation of quantum-size structures.

Acknowledgements. This work was supported by the European Commission (Project FP-6 IST-4, Contract No. 027976) and the Presidium of the Russian Academy of Sciences (Basic Research Programme No. 27).

References

1. Ledentsov N.N., Ustinov V.M., Shchukin V.A., et al. *Fiz. Tekh. Poluprovodn.*, **32**, 385 (1998).
2. Roko M.C., Williams R.S., Alivisatos P. (Eds) *Nanotechnology Research Directions: Vision for Nanotechnology in the Next Decade* (Boston: Kluwer, 2000; Moscow: Mir, 2002) p. 293.
3. Ustinov V.M. *Fiz. Tekh. Poluprovodn.*, **38**, 963 (2004).
4. Kryzhanovskaya N.V., Gladyshev A.G., Blokhin S.A., et al. *Fiz. Tekh. Poluprovodn.*, **38**, 867 (2004).
5. Zvonkov B.N., Karpovich I.A., Baidus' N.V., et al. *Fiz. Tekh. Poluprovodn.*, **35**, 92 (2001).
6. Sgartato A., Szkutnik P.D., Balzarotti A., Motta N., Rosel F. *Appl. Phys. Lett.*, **83**, 4002 (2004).

7. Placidi E., Della Pia A., Arciprete F. *Appl. Phys. Lett.*, **94**, 021901 (2009).
8. Kitajima T., Lu B., Leone S.R. *Appl. Phys. Lett.*, **80**, 497 (2002).
9. Capellini G., De Seta M., Spinella C., Evangelisti F. *Appl. Phys. Lett.*, **82**, 1772 (2003).
10. Zhoug Z., Halilovic A., Fromherz T., Schaffer F., Bauer G. *Appl. Phys. Lett.*, **82**, 4779 (2003).
11. Li Q., Han S.M., Brueck S.R.J., Hersee S., Jiang Y.-B. *Appl. Phys. Lett.*, **83**, 5032 (2003).
12. Alonso-Gonzalez P., Gonzalez L., Gonzalez Y., Fuster D., Fernandez-Martinez I., Martin-Sanchez J., Abelmann L. *Nanotechnology*, **18**, 355302 (2007).
13. Pedraza A.J., Fowlkes J.D., Guan Y.-F. *Appl. Phys. A*, **77**, 277 (2003).
14. Patella F., Szkutnik A., Sgarlata E. *J. Phys.: Condens. Matter.*, **16**, S1503 (2004).
15. Lee J.H., Wang Zh.M., Liang B.L., Sablon K.A., Strom N.W., Salamo G.J. *Semicond. Sci. Technol.*, **21**, 1547 (2006).
16. Liang B.L., Wang Zh.M., Lee J.H., Sablon K.A., Mazur Yu.I., Salamo G.J. *Appl. Phys. Lett.*, **89**, 213103 (2006).
17. Verevkin Yu.K., Daume E.Ya., Petryakov V.N., Gushchina Yu.Yu., Tikhov S.V. *Pis'ma Zh. Tekh. Fiz.*, **31** (17), 83 (2005).
18. Fernandez A., Phillion D.W. *Appl. Opt.*, **37** (3), 473 (1998).
19. Alekseev A.M., Verevkin Yu.K., Vostokov N.V., et al. *Pis'ma Zh. Eksp. Teor. Fiz.*, **73** (4), 214 (2001).
20. Bredikhin V.I., Verevkin Yu.K., Daume E.Ya., et al. *Kvantovaya Elektron.*, **30**, 333 (2000) [*Quantum Electron.*, **30**, 333 (2000)].
21. Verevkin Yu.K., Bronnikova N.G., Korolikhin V.V., et al. *Zh. Tekh. Fiz.*, **73**, 99 (2003).
22. Bredikhin V.I., Burenina V.N., Verevkin Yu.K., et al. *Zh. Tekh. Fiz.*, **74**, 86 (2004).